Case Studies in Thermal Engineering 4 (2014) 202–214

Contents lists available at ScienceDirect

Case Studies in Thermal Engineering

journal homepage: www.elsevier.com/locate/csite

# Scrutiny of underdeveloped nanofluid MHD flow and heat conduction in a channel with porous walls

M. Fakour [a,*], D.D. Ganji [b], M. Abbasi [a]

[a] Department of Mechanical Engineering, Sari Branch, Islamic Azad University, Sari, Iran
[b] Department of Mechanical Engineering, Babol University of Technology, Babol, Iran

ARTICLE INFO

*Article history:*
Received 8 October 2014
Accepted 19 October 2014
Available online 28 October 2014

*Keywords:*
Least square method (LSM)
Laminar viscous flow
Heat transfer
Uniform magnetic field
Channel with porous walls

ABSTRACT

In this paper, laminar fluid flow and heat transfer in channel with permeable walls in the presence of a transverse magnetic field is investigated. Least square method (LSM) for computing approximate solutions of nonlinear differential equations governing the problem. We have tried to show reliability and performance of the present method compared with the numerical method (Runge–Kutta fourth-rate) to solve this problem. The influence of the four dimensionless numbers: the Hartmann number, Reynolds number, Prandtl number and Eckert number on non-dimensional velocity and temperature profiles are considered. The results show analytical present method is very close to numerically method. In general, increasing the Reynolds and Hartman number is reduces the nanofluid flow velocity in the channel and the maximum amount of temperature increase and increasing the Prandtl and Eckert number will increase the maximum amount of theta.



## 1. Introduction

Flow problem in a porous tube or channel received much attention in recent years due to its various applications in medical engineering, for example, in the dialysis of blood in artificial kidney [1], in the flow of blood in the capillaries [2], in the flow in blood oxygenators [3], as well as in many other engineering areas such as the design of filters [4], in transpiration cooling boundary layer control [5] and gaseous diffusion [6]. In 1953, Berman [7] described an exact solution of the Navier–Stokes equation for steady two-dimensional laminar flow of a viscous, incompressible fluid in a channel with parallel, rigid, porous walls driven by uniform, steady suction or injection at the walls. This mass transfer is paramount in some industrial processes. More recently, Rashidi and et al. [8] Homotopy Simulation of Nanofluid Dynamics from a non-linearly stretching isothermal permeable sheet with Transpiration investigated.

Slow viscous flow problem in a semi-porous channel in the presence of transverse magnetic field is investigated by Sheikholeslami et al. [9]. They show that the method is asymptotically optimal Homotopy a powerful method for solving nonlinear differential equations, such as the problem. Soleimani et al. [10] studied of natural convection heat transfer in an enclosure filled mid-loop with nanofluid using the control volume based Finite Element Method. They founded turn angle has a significant effect on flow lines, isotherms and local Nusselt number is maximum or minimum values. Sheikholeslami

* Corresponding author. Tel.: +989119579177.
*E-mail addresses:* mehdi_fakour@yahoo.com, mehdi_fakoor8@yahoo.com (M. Fakour), ddg_davood@yahoo.com (D.D. Ganji), mmmortezaabbasi@gmail.com (M. Abbasi).

http://dx.doi.org/10.1016/j.csite.2014.10.003

**Nomenclature**

| | |
|---|---|
| NUM | numerical method |
| $P$ | pressure |
| $q$ | mass transfer parameter |
| $Re$ | Reynolds number |
| $U$ | dimensionless velocity in the $x$ direction |
| $V$ | dimensionless velocity in the $y$ direction |
| $h$ | suspension height |
| $Ec$ | Eckert number |
| $Ha$ | Hartmann number |
| $Pr$ | Prandtl number |
| $L_x$ | length of the slider |
| $C_p$ | specific heat |
| $k$ | thermal conductivity |
| $\Delta T = T_h - T_0$ | difference temperature between the plates |
| $u_0$ | $x$ velocity of the pad |
| $u$ | dimensionless $x$—component velocity |
| $v$ | dimensionless $y$—component velocity |
| $u^*$ | velocity component in the $x$ direction |
| $v^*$ | velocity component in the $y$ direction |
| $x$ | dimensionless horizontal coordinate |
| $y$ | dimensionless vertical coordinate |
| $x^*$ | distance in the $x$ direction parallel to the plates |
| $y^*$ | distance in the $y$ direction parallel to the plates |

*Greek symbols*

| | |
|---|---|
| $\rho$ | fluid density |
| $\theta$ | dimensionless temperature |
| $\nu$ | kinematic viscosity |
| $\sigma$ | electrical conductivity |
| $\varepsilon$ | aspect ratio $h/Lx$ |
| $\alpha$ | fluid thermal diffusivity |

*Abbreviations of LSM*

| | |
|---|---|
| LSM | least square method |
| $D$ | differential operator |
| $u$ | estimated by a function |
| $\tilde{u}$ | linear combination of fundamental functions |
| $R$ | residual |
| $W_i$ | weight functions |

et al. [11] investigated the flow of nanofluid and heat transfer characteristics between two horizontal plates in a rotating system. Their results showed that for suction and injection, the heat transfer rate increases with the nanoparticle volume fraction, Reynolds number, and parameter injection / suction increases and then decreases with the strength of the spin parameter. Simultaneous effects of partial slip and thermal-diffusion and diffusion-thermo on steady MHD Convective Flow due to a Rotating Disk studied by Rashidi et al. [12]. Natural convection of a non-Newtonian copper–water nanofluid between two infinite parallel vertical flat plates was investigated by Domairry et al. [13]. They concluded that as the size of nanoparticles increases, the boundary layer thickness increases, the thermal boundary layer thickness decreases. Sheikholeslami et al. [14] studied the natural convection in a concentric annulus between a cold outer square and heated inner circular cylinders in the presence of static radial magnetic field. Sheikholeslami et al. [15] performed a numerical analysis for natural convection heat transfer of Cu–water nanofluid in a cold outer circular enclosure containing a hot inner sinusoidal circular cylinder in the presence of horizontal magnetic field using the control volume based Finite Element Method. They concluded that in the absence of a magnetic field, increasing the Rayleigh number increases, while the opposite trend was observed in the presence of a magnetic field decreases. Sheikholeslami et al. [16] studied the effects of magnetic field and nanoparticle on the Jeffery–Hamel flow using Adomian decomposition method. They showed that increasing Hartmann number will lead to backflow reduction. Recently several authors investigated about nanofluid flow and heat transfer [17–20].

The main goal of this paper is to examine the laminar nanofluid flow in channel with permeable walls in the presence of transverse magnetic field using least square method. Effective Hartmann number, Reynolds number, Prandtl number, and Eckert number on the velocity and temperature considered. In addition to speed and temperature for different structures nanofluid (copper and silver nanoparticles in water or ethylene glycol) depicted.

## 2. Problem description

Steady two-dimensional laminar flow of an incompressible viscous electrically conducting fluid in a channel with permeable walls with a long rectangular plate with uniform translation in $x^*$, $L_x$ over an infinite porous plate and made to consider. The distance between the two plates is $h$. We are observing a normal velocity $q$ on the porous walls (Fig. 1). A uniform magnetic field $B$ is assumed to be applied towards direction $y^*$.

In the case of a short circuit to neglect the electrical field and perturbations to the basic normal field and without any gravity forces, the governing equations are [19]:

$$\frac{\partial u^*}{\partial x^*}+\frac{\partial v^*}{\partial y^*}=0, \tag{1}$$

$$u^*\frac{\partial u^*}{\partial x^*}+v^*\frac{\partial u^*}{\partial y^*}=-\frac{1}{\rho_{nf}}\frac{\partial P^*}{\partial x^*}+\nu_{nf}\left(\frac{\partial^2 u^*}{\partial x^{*2}}+\frac{\partial^2 u^*}{\partial y^{*2}}\right)-u^*\frac{\sigma_{nf}B^2}{\rho_{nf}}, \tag{2}$$

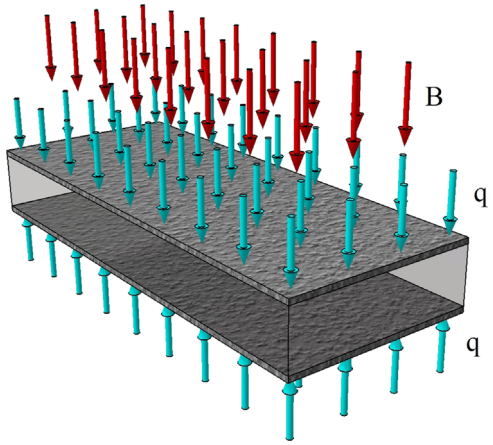


**Fig. 1.** Three dimensional Schematic of the problem water with copper, $Re=Ha=Ec=1$, $Pr=5.784$, $\varphi=0.04$.

$$u^*\frac{\partial v^*}{\partial x^*}+v^*\frac{\partial v^*}{\partial y^*}=-\frac{1}{\rho_{nf}}\frac{\partial P^*}{\partial y^*}+\nu_{nf}\left(\frac{\partial^2 v^*}{\partial x^{*2}}+\frac{\partial^2 v^*}{\partial y^{*2}}\right). \tag{3}$$

$$\rho_{nf}\times C_p\left(u^*\frac{\partial T}{\partial x^*}+v^*\frac{\partial T}{\partial y^*}\right)=k_{nf}\left(\frac{\partial^2 T}{\partial x^{*2}}+\frac{\partial^2 T}{\partial y^{*2}}\right)+\mu_{nf}\left(\frac{\partial u^*}{\partial y^*}\right)^2 \tag{4}$$

The suitable boundary conditions for the velocity and temperature are:

$$\begin{aligned} &y^*=0: u^*=0, T=T_o\\ &v^*=q \end{aligned} \tag{5}$$

$$\begin{aligned} &y^*=h: u^*=u_0, T=T_h\\ &v^*=-q \end{aligned} \tag{6}$$

Calculating a mean velocity $U$ by the relation:

$$U\times h=\int_0^h u^*\times dy^*=L_x\times q \tag{7}$$

We consider the following transformations:

$$x=\frac{x^*}{L_x},\quad y=\frac{y^*}{h},\quad u=\frac{u^*}{U},\quad v=\frac{v^*}{q},\quad P_y=\frac{P^*}{\rho\times q^2},\quad \theta=\frac{T-T_o}{T_h-T_o} \tag{8}$$

Then, we can consider four dimensionless numbers: the Hartmann number $Ha$ for the description of magnetic forces [11] and the Reynolds number $Re$ for dynamic forces, Prandtl number and Eckert number:

$$Ha=Bh\sqrt{\frac{\sigma_f}{\rho_f\times\nu_f}}, \tag{9}$$

$$\mathrm{Re}=\frac{hq}{\nu_{nf}} \tag{10}$$

$$\mathrm{Pr}=\frac{\mu_{nf}C_p}{k_{nf}} \tag{11}$$

$$Ec=\frac{U^2}{C_p(T_h-T_o)} \tag{12}$$

where the effective density ($\rho_{nf}$) and specific heat capacity ($C_P$) are defined as [12]:

$$\begin{aligned} &\rho_{nf}=\rho_f(1-\phi)+\rho_s\phi\\ &(\rho.C_p)_{nf}=(\rho\times C_p)_f(1-\phi)+(\rho\times .C_p)_s\phi \end{aligned} \tag{13}$$

The effective thermal conductivity of the nanofluid can be approximated by the Maxwell–Garnett's (MG) model as [13]:

$$\frac{k_{nf}}{k_f}=\frac{k_s+2k_f-2\phi(k_f-k_s)}{k_s+2k_f+\phi(k_f-k_s)} \tag{14}$$

**Table 1**
Different models for simulation of dynamic viscosity.

| Model | Thermal conductivity | Dynamic viscosity |
|---|---|---|
| I | $\frac{\sigma_{nf}}{\sigma_f}=1+\frac{3(\sigma_s/\sigma_f-1)\phi}{(\sigma_s/\sigma_f+2)-(\sigma_s/\sigma_f-1)\phi}$ | $\mu_{nf}=\frac{\mu_f}{(1-\phi)^{2.5}}$ |
| II | $\frac{\sigma_{nf}}{\sigma_f}=1+\frac{3(\sigma_s/\sigma_f-1)\phi}{(\sigma_s/\sigma_f+2)-(\sigma_s/\sigma_f-1)\phi}$ | $\mu_{nf}=\mu_f(1+7.3\phi+123\phi^2)$ |

**Table 2**
Thermo physical properties of nanofluids and nanoparticles.

| Material | Density ($\rho$) | Electrical conductivity ($\sigma$) | Specific heat capacity ($C_P$) | Thermal conductivity (K) |
|---|---|---|---|---|
| **Silver** | 10500 | $6.30\times10^7$ | 230 | 418 |
| **Copper** | 8933 | $5.96\times10^7$ | 385 | 401 |
| **Ethylene glycol** | 1113.2 | $1.07\times10^{-4}$ | 2410 | 0.252 |
| **Drinking water** | 997.1 | 0.05 | 4179 | 0.613 |

where $\phi$ is the nanoparticle volume fraction. Different models for simulating dynamic viscosity of the nanofluids are shown in Table 1. In the first model, the effective thermal conductivity and viscosity of nanofluid are calculated by the Maxwell [13], [18] and Brinkman models, respectively. The thermo physical properties of the nanofluid are given in Table 2.

Introducing Eqs. (7)–(12) into Eqs. (1)–(4) leads to the dimensionless equations:

$$\frac{\partial u}{\partial x}+\frac{\partial v}{\partial y}=0, \tag{15}$$

$$u\frac{\partial u}{\partial x}+v\frac{\partial u}{\partial y}=-\varepsilon^2\frac{\partial P_y}{\partial x}+\frac{\nu_{nf}}{hq}\left(\varepsilon^2\frac{\partial^2 u}{\partial x^2}+\frac{\partial^2 u}{\partial y^2}\right)-u\frac{Ha^2}{\mathrm{Re}}\frac{B^*}{A^*}, \tag{16}$$

$$u\frac{\partial v}{\partial x}+v\frac{\partial v}{\partial y}=-\frac{\partial P_y}{\partial y}+\frac{\nu_{nf}}{hq}\left(\varepsilon^2\frac{\partial^2 v}{\partial x^2}+\frac{\partial^2 v}{\partial y^2}\right) \tag{17}$$

$$\frac{C^*}{D^*}\mathrm{Pr}\left[\mathrm{Re}\left(u\frac{\partial\theta}{\partial x}+v\frac{\partial\theta}{\partial y}\right)-Ec\left(\frac{\partial u}{\partial y}\right)^2\right]=\varepsilon^2\left(\frac{\partial^2\theta}{\partial x^2}+\frac{\partial^2\theta}{\partial y^2}\right) \tag{18}$$

where $A^*$, $B^*$, $C^*$ and $D^*$ are constant parameters:

$$A^*=(1-\phi)+\frac{\rho_s}{\rho_f}\phi,\quad B^*=1+\frac{3(\sigma_s/\sigma_f-1)\phi}{(\sigma_s/\sigma_f+2)-(\sigma_s/\sigma_f-1)\phi} \tag{19}$$

$$C^*=\frac{k_s+2k_f-2\phi(k_f-k_s)}{k_s+2k_f+\phi(k_f-k_s)},\quad D^*=(1-\phi)+\frac{(\rho.\,C_p)_s}{(\rho.\,C_p)_f}\phi \tag{20}$$

Quantity of $\varepsilon$ is defined as the aspect ratio between distance $h$ and a characteristic length $L_x$ of the slider. This ratio is normally small. Berman's similarity transformation is used to be free from the aspect ratio of $\varepsilon$:

$$v=-V(y),u=\frac{u^*}{U}=u_0\times U(y)+x\frac{dV}{dy}. \tag{21}$$

Introducing Eq. (21) in the second momentum Eq. (17) shows that quantity $\partial P_y/\partial y$ does not depend on the longitudinal variable $x$. With the first momentum equation, we also observe that $\partial^2 P_y/\partial x^2$ is independent of $x$. We omit asterisks for simplicity. Then a separation of variables leads to [11]:

$$UV'-VU'=\frac{1}{\mathrm{Re}}\frac{1}{A^*(1-\phi)^{2.5}}\left[U''-Ha^2B^*(1-\phi)^{2.5}U\right] \tag{22}$$

$$V^{IV}=Ha^2B^*(1-\phi)^{2.5}V''+\mathrm{Re}A^*(1-\phi)^{2.5}\left[V'V''-VV'''\right] \tag{23}$$

$$\theta''=-\frac{C^*}{D^*}(1-\phi)^{2.5}\mathrm{Pr}\left(\mathrm{Re}(1-\phi)^{2.5}V\theta'+Ec(u_0U')^2\right) \tag{24}$$

where primes denote differentiation with respect to y and asterisks have been omitted for simplicity. The dynamic boundary conditions are:

$$\begin{aligned} &y=0: U=0, \quad V'=0, \quad \theta=0 \\ &V=-1 \\ &y=1: U=1, \quad V'=0, \quad \theta=1 \\ &V=1 \end{aligned} \tag{25}$$

## 3. Describe least square method and applied to the problem

*Describe least square method*

As Sheikholeslami, Hatami and Ganji [19] defined least square method is one of the weighted residual methods which are constructed on minimizing the residuals of the trial function introduced to the nonlinear differential equation.

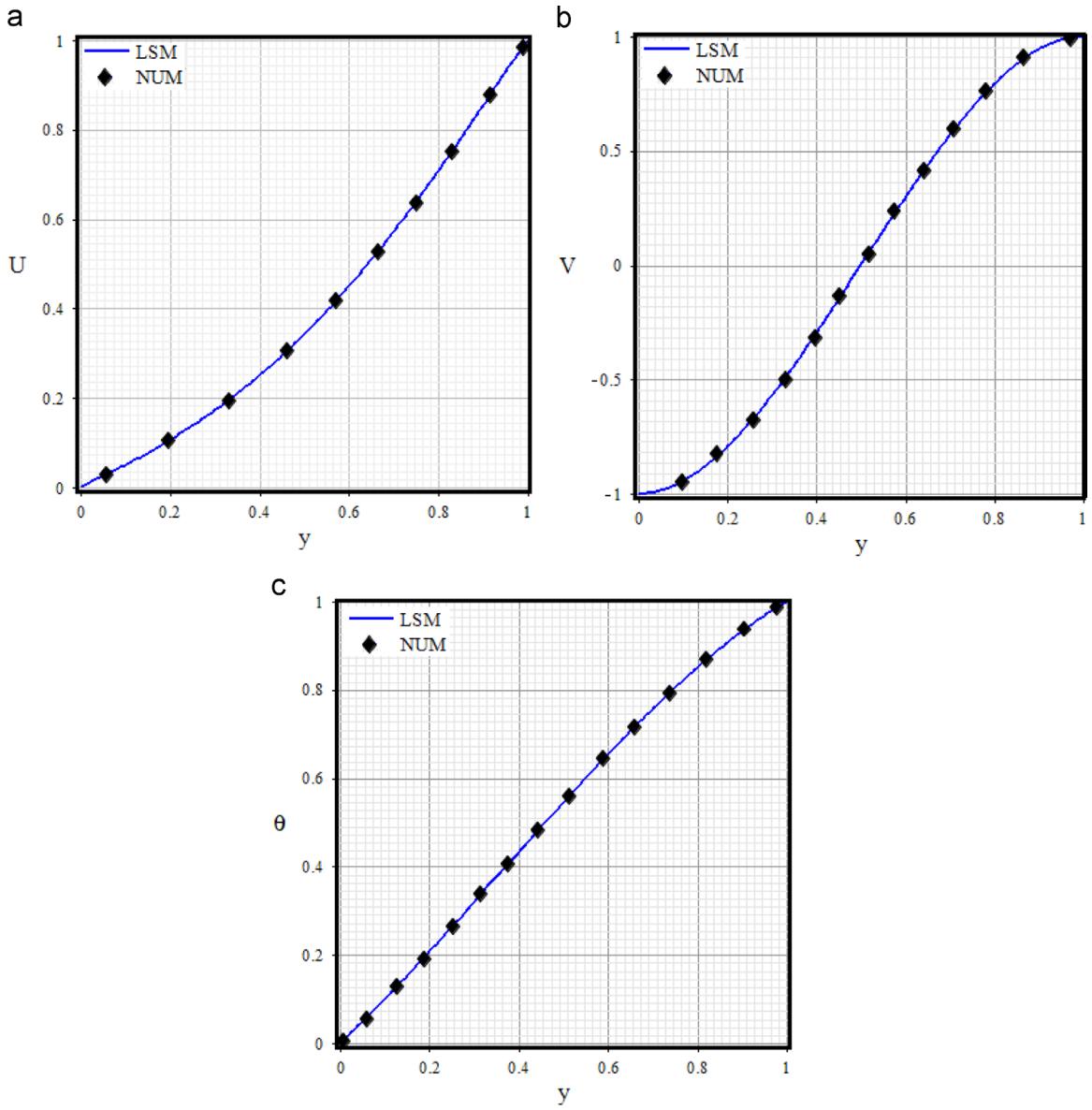


**Fig. 2.** Comparison of LSM and numerical results for dimensionless velocities and temperature (a) $U(y)$, (b) $V(y)$ and (c) $\theta\theta(y)$.

For perception the principle of LSM, consider a differential operator $D$ is acted on a function $u$ to produce a function $p$:

$$D(u(x)) = p(x) \tag{26}$$

It is considered that $u$ is estimated by a function, $\tilde{u}$ which is a linear combination of fundamental functions chosen from a linearly independent set. This is,

$$u \cong \tilde{u} = \sum_{i=1}^{n} c_i \varphi_i \tag{27}$$

by substituting Eq. (27) into the differential operator, D, the result of the operations generally isn't $p(x)$ and a difference will be appeared. Hence an error or residual will exist as follows:

$$R(x) = D(\tilde{u}(x)) - p(x) \neq 0 \tag{28}$$

The main concept of LSM is to force the residual to zero in some average sense over the domain. So,

$$\int_x R(x) W_i(x) = 0 \quad i = 1, 2, \ldots, n \tag{29}$$

where the number of weight functions $W_i$, is accurately equal the number of unknown coefficients $c_i$ in$\tilde{u}$. The result is a set of $n$ algebraic equations for the undefined coefficients $c_i$. If the continuous summation of all the squared residuals is minimized, the rationale behind the LSM's name can be seen. In other words, a minimum of

$$S = \int_x R(x) R(x) dx = \int_x R^2(x) dx \tag{30}$$

In order to achieve a minimum of this function Eq. (30), the derivatives of $S$ with respect to all the each unknown parameter should be zero. i.e.

$$\frac{\partial S}{\partial c_i} = 2 \int_x R(x) \frac{\partial R}{\partial c_i} dx = 0 \tag{31}$$

Comparing with Eq. (31), the weighted functions for LSM will be,

$$W_i = 2 \frac{\partial R}{\partial c_i} \tag{32}$$

Because the "2" coefficient can be eliminated, it can be negligible in the equation. So the weighted functions, $W_i$, for the least squares method are the derivatives of the residuals with respect to the unknown constants

$$W_i = \frac{\partial R}{\partial c_i} \tag{33}$$

**Table 3**
Comparison between $V(y)$, $U(y)$ and $\theta\,\theta(y)$ results from applied method for $Re = Ha = 1$ and $\varphi = 0.04$.

| $Y$ | LSM($U$) | LSM(V) | LSM($\theta$) | NUM() | NM(V) | NUM($\theta$) |
|---|---|---|---|---|---|---|
| 0.00 | 0.000000000 | −1.000000000 | 0.000000000 | 0.000000000 | −1.000000000 | 0.000000000 |
| 0.05 | 0.022427956 | 0.9883224964 | 0.48923410 | 0.022428461 | −0.9883236955 | 0.048923122 |
| 0.10 | 0.048138764 | −0.9530069690 | 0.09974320 | 0.048144234 | −0.9530054561 | 0.09997954 |
| 0.15 | 0.077069004 | −0.8943169260 | 0.152817031 | 0.077069152 | −0.8943159841 | 0.152816522 |
| 0.20 | 0.109155251 | −0.8133498534 | 0.207115856 | 0.109156431 | −0.8133489574 | 0.207115214 |
| 0.25 | 0.144334085 | −0.7119329689 | 0.262535090 | 0.144335684 | −0.7119325463 | 0.262534652 |
| 0.30 | 0.182542084 | −0.5925189741 | 0.318739042 | 0.182543145 | −0.5925185463 | 0.318738641 |
| 0.35 | 0.223715825 | −0.4580818070 | 0.375392014 | 0.223717125 | −0.4580817984 | 0.375391748 |
| 0.40 | 0.267791886 | −0.3120123949 | 0.432158311 | 0.267792453 | −0.3120120014 | 0.432157743 |
| 0.45 | 0.314706846 | −0.1580144071 | 0.488702238 | 0.314707124 | −0.1580141225 | 0.488701985 |
| 0.50 | 0.364397282 | 0.0000000000 | 0.544688099 | 0.364398164 | 0.0000000000 | 0.544687685 |
| 0.55 | 0.416799773 | 0.1580143920 | 0.599780198 | 0.416799842 | 0.1580140123 | 0.599780184 |
| 0.60 | 0.471850896 | 0.3120123796 | 0.653642839 | 0.471851123 | 0.3120123458 | 0.653642398 |
| 0.65 | 0.529487229 | 0.4580817941 | 0.705940326 | 0.529488259 | 0.4580817455 | 0.705940128 |
| 0.70 | 0.589645350 | 0.5925189616 | 0.756336965 | 0.589646384 | 0.5925189423 | 0.756336325 |
| 0.75 | 0.652261838 | 0.7119329594 | 0.804497058 | 0.652262287 | 0.7119325664 | 0.804496845 |
| 0.80 | 0.717273270 | 0.8133498466 | 0.850084910 | 0.717274598 | 0.81334954471 | 0.850084521 |
| 0.85 | 0.784616224 | 0.894316920 | 0.892764826 | 0.784617021 | 0.8943165412 | 0.892764430 |
| 0.90 | 0.854227278 | 0.953006964 | 0.932201111 | 0.854228137 | 0.9530061223 | 0.932200147 |
| 0.95 | 0.926043011 | 0.988322493 | 0.968058067 | 0.926054831 | 0.9883221447 | 0.968057752 |
| 1.00 | 1.000000000 | 1.0000000000 | 1.000000000 | 1.000000000 | 1.0000000000 | 1.000000000 |

*The LSM applied to the problem*

It should be noted that the trial solution must satisfies the boundary conditions, and Eqs. (34)–(36), since the boundary conditions are assumed to apply them [20] so the trial solution can be written as

$$U(y) = y + c_1(y - y^2) + c_2(y - y^3) \tag{34}$$

$$V(y) = -1 + c_3\left(\frac{y^2}{2} - \frac{y^3}{3}\right) + c_4\left(\frac{y^2}{2} - \frac{y^4}{4}\right) + c_5\left(\frac{y^2}{2} - \frac{y^5}{5}\right) \tag{35}$$

$$\theta(y) = y + c_6(y - y^2) + c_7(y - y^3) \tag{36}$$

By introducing this equation to Eqs. (22)–(24) residual function will be found and by substituting the residual function into Eqs. (34)–(36) a set of equations with seven equations and seven unknown coefficients will be appeared and by solving

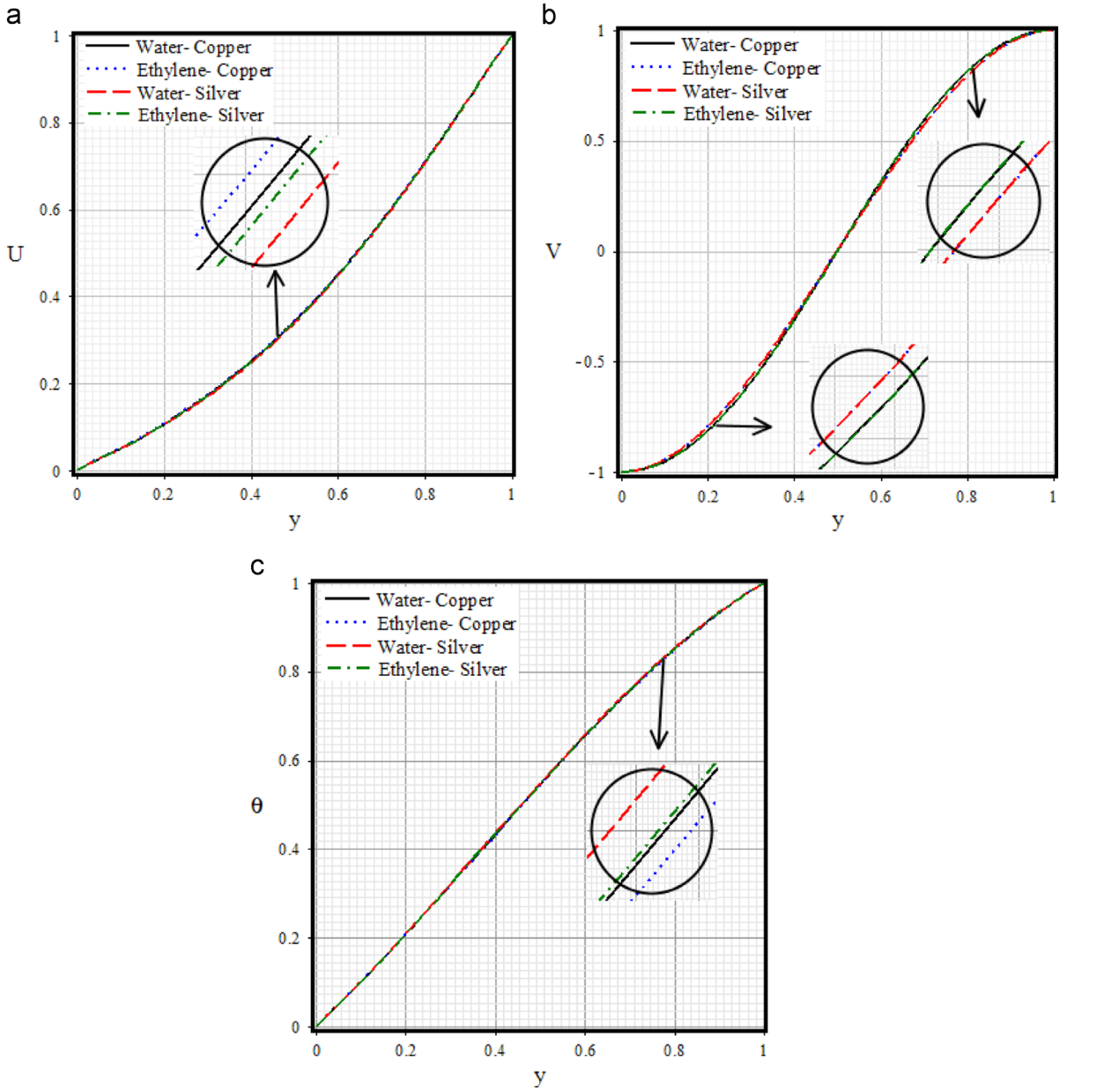


**Fig. 3.** The effects of the nanoparticle and liquid phase material on velocity and temperature's profiles.

this system of equations, coefficients $c1$–$c7$ will be determined. By using LSM, when $Re=1$, $Ha=1$, $Pr=5.784$, $Ec=1$, $\varphi=0.04$, $u_0=1$, $A^*=1.318359242$, $B^*=1.125$, $C^*=1.124404794$ and $D^*=0.9930146705$ following equations will be determined for temperature distribution and velocities for laminar nanofluid flow in channel with permeable walls in the presence of a transverse magnetic field.

$$U(y)=0.4153077844y+0.6692549096y^2-0.0845626943y^3 \tag{37}$$

$$V(y)=-1+4.610035778y^2+1.559856294y^3-6.949819942y^4+2.779927864y^5 \tag{38}$$

$$\theta(y)=0.9549552385y+0.4926390805y^2-0.4475943189y^3 \tag{39}$$

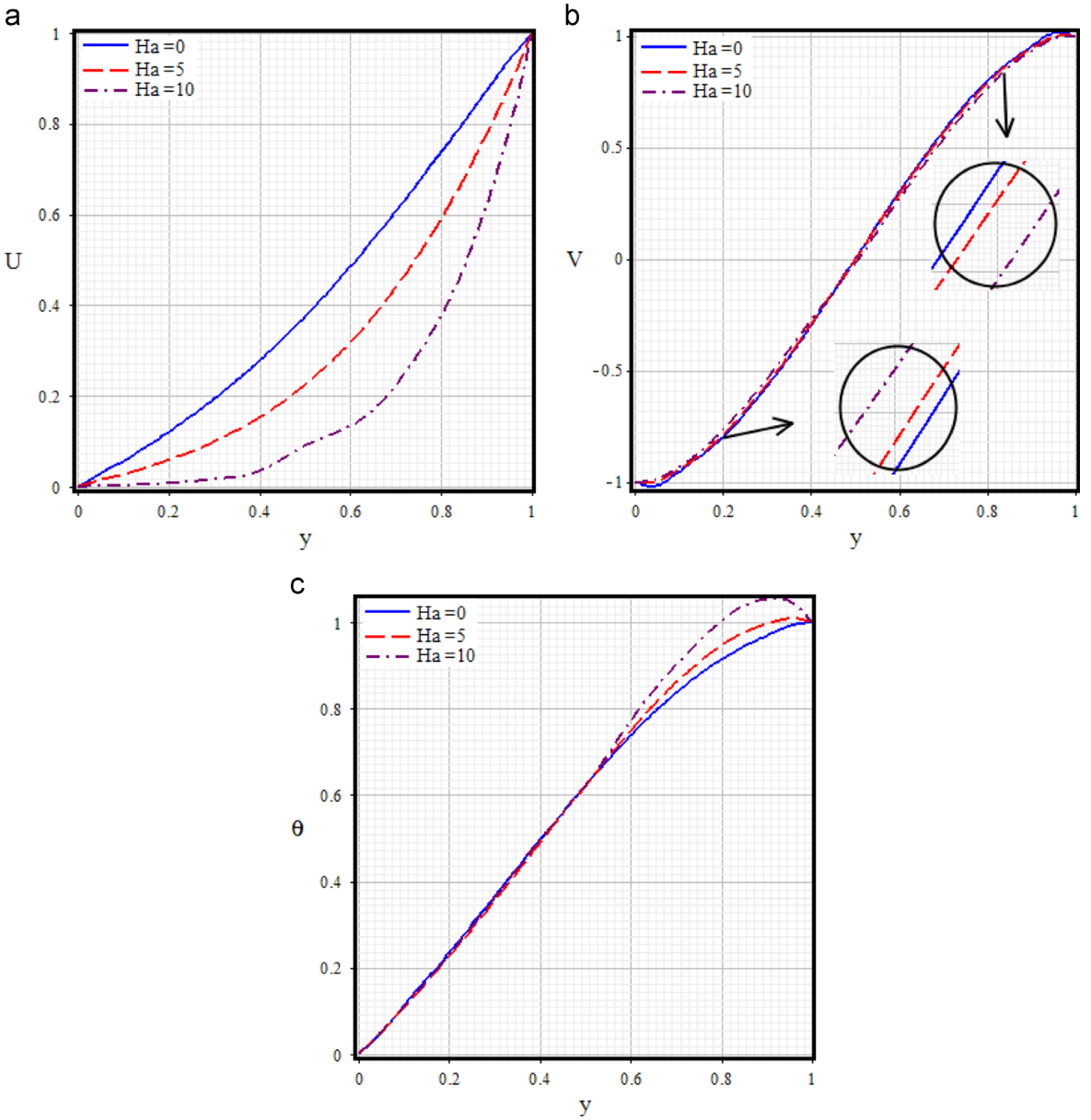


**Fig. 4.** Effect of Hartmann number ($Ha$) on dimensionless velocities and temperature for water with copper nanoparticles, $\varphi=0.04$, (a) $V(y)$, $Re=1$, (b) $U(y)$, $Re=1$, (c) $\theta\theta(y)$, $Re=Ec=1$, $Pr=5.784$. (d) $V(y)$, $Re=5$, (e) $U(y)$, $Re=5$, (f) $\theta(y)$, $Re=Ec=5$, $Pr=5.784$.

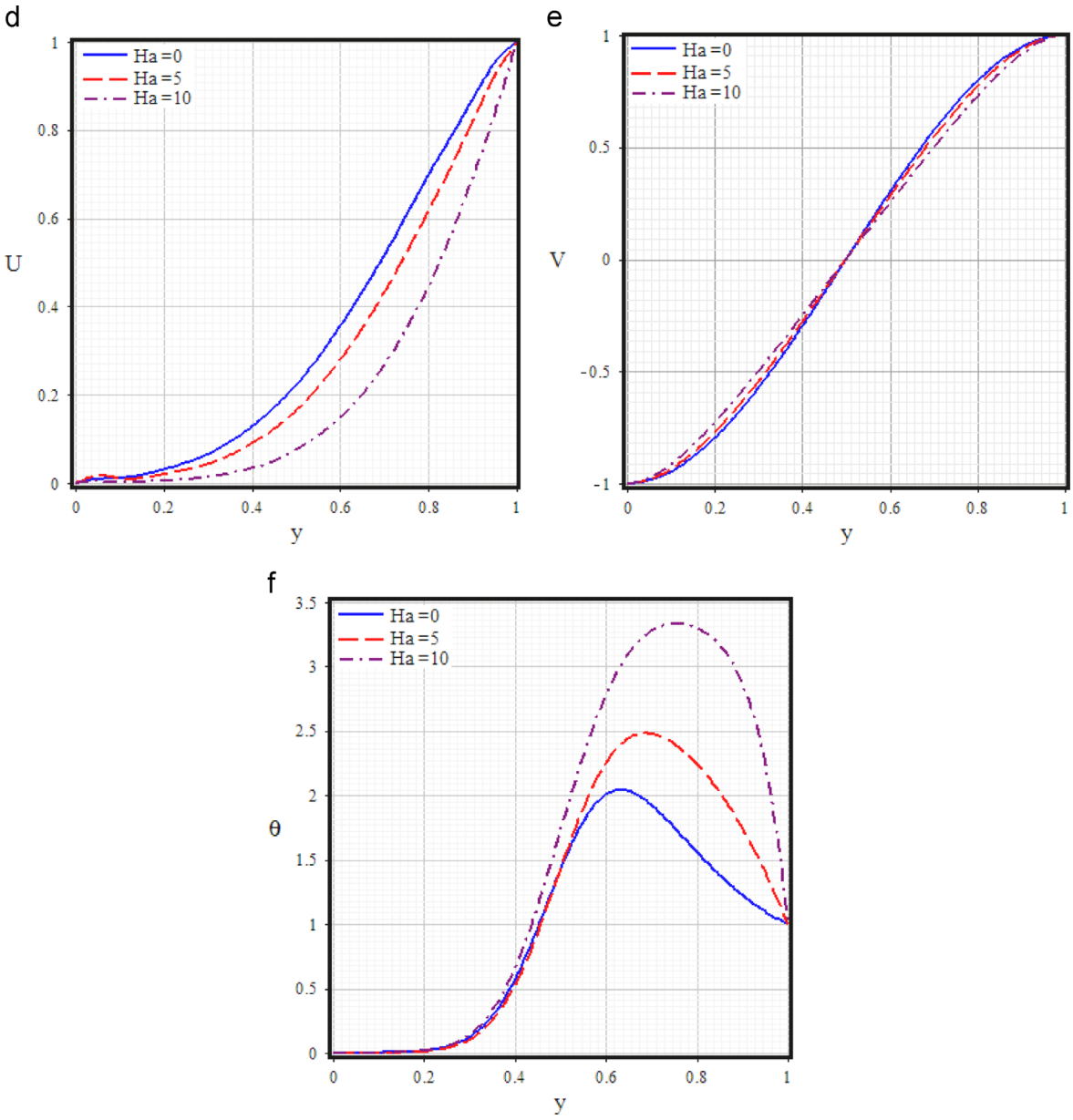


**Fig. 4.** (*continued*)

## 4. Results and discussion

In the present study LSM method is applied to obtain an explicit analytic solution of the laminar nanofluid flow and heat transfer in a channel with porous walls in the presence of uniform magnetic field (Fig. 1). First, in Fig. 2 the comparison between the present method and numerical method to solve this problem for Cu–water nanofluid has been shown. Comparison between analytical and numerical methods for $U$, $V$ and $\theta$ are provided in Table 3. As is observed the presented analytical method is a valid and powerful method to solve this kinds of problems in science and engineering. The effects of the nanoparticle and liquid phase material on velocity's profiles are shown in Fig. 3. This figure reveals that when nanofluid includes copper (as nanoparticles) or ethylene glycol (as fluid phase) in its structure, the $U(y)$ value is greater than the other structures. Effects of magnetic field on the temperature and velocity profiles are shown in Fig. 4. Generally, when the magnetic field is imposed on the enclosure, the velocity field suppressed owing to the retarding effect of the Lorenz force. Also the maximum value of $\theta$ increases because of Hartman number increases. For example for low Reynolds number, as Hartmann number increases $V(y)$ decreases for $y > y_m$ but opposite trend is observed for $y < y_m$, $y_m$ is a meeting point that

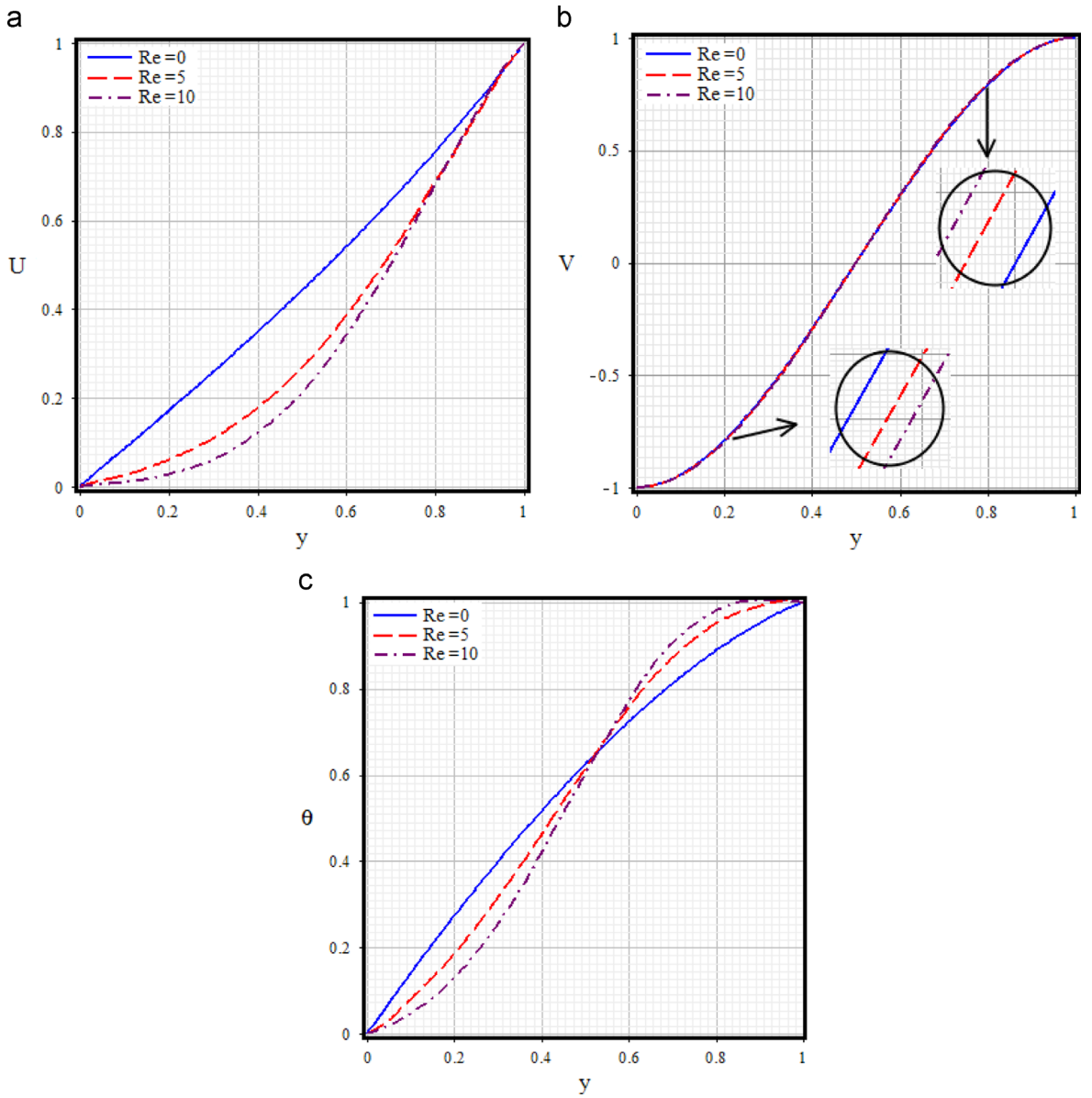


**Fig. 5.** Effect of Reynolds number (*Re*) on dimensionless velocities and temperature for water with copper nanoparticles, $\varphi=0.04$, (a) $V(y)$, $Ha=1$, (b) $U(y)$, $Ha=1$, (c) $\theta(y)$, $Ha=Ec=1$, $Pr=5.784$ (d) $V(y)$, $Ha=10$, (e) $U(y)$, $Ha=10$, (f) $\theta(y)$, $Ha=Ec=10$, $Pr=5.784$.

all curves joint together at this point. Also it is worth to mention that the maximum value of $\theta$ happens in $Re=Ec=5$, $Pr=5.784$, $Ha=10$. Effects of Reynolds number on the temperature and velocity profiles are shown in Fig. 5. The velocity profile $V(y)$ is not affected by Reynolds number changes. For low Hartman number, as Reynolds number increases. For high Hartman number, as Hartmann number increases $V(y)$ decreases for $y>y_m$ but opposite trend is observed for $y<y_m$. It is worth to mention that the Reynolds number indicates the relative significance of the inertia effect compared to the viscous effect and in turn increasing *Re* leads to an increase in the magnitude of the skin friction coefficient. For low *Ha*, *Pr* and *Ec* number, as Reynolds number increases temperature increases for $y>y_m$ but opposite trend is observed for $y<y_m$. For high *Ha*, *Pr* and *Ec* number, as Reynolds number increases maximum magnitude of temperature decreases. Effect of Prandtl number on the temperature profile is shown Fig. 6. Generally, with increasing of Prandtl number, the maximum value of theta increases in channel and the maximum value of $\theta$ occurs at $Ha=Re=Ec=10$, $Pr=7.923$. Fig. 6 shows the effects of Eckert number on the temperature profile. Generally, increasing the Eckert number, the maximum value of theta increases and maximum value of $\theta$ occurs at $Ha=Re=Ec=10$. In all above result model I was used for simulating $\mu_{nf}$.

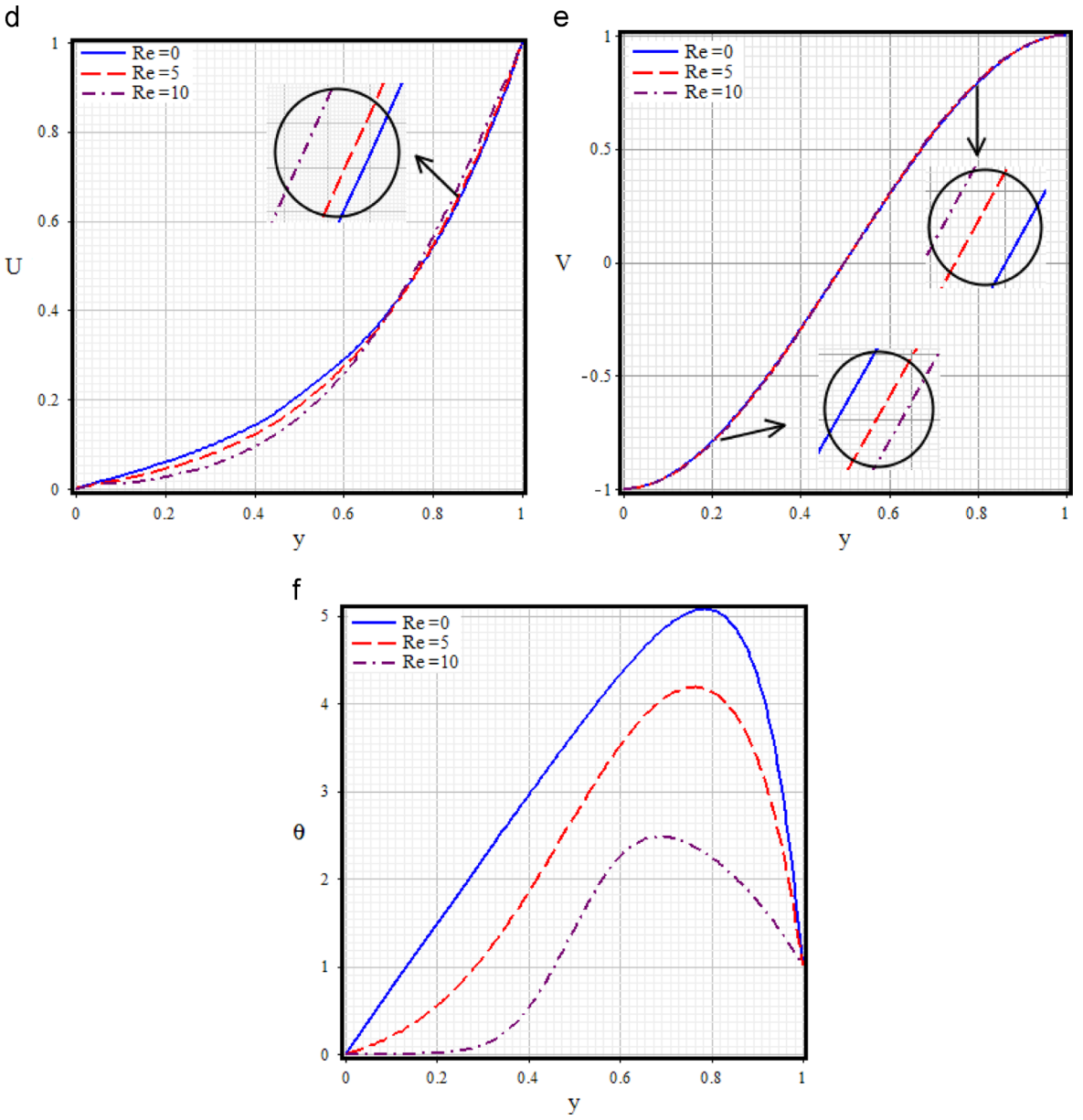


**Fig. 5.** (*continued*)

## 5. Conclusion

In this study, least square method is applied to solve the problem of laminar nanofluid flow and heat transfer in a channel with porous walls in the presence of uniform magnetic field. First of all a comparison between the applied method, LSM and Numerical method is investigated. The results indicate that least square method has a good agreement with numerically results. By solution of this equation the following points is concluded:

- In general, by applied magnetic field, velocity in the channel is reduced and the maximum amount of temperature increases.
- Increasing of Reynolds number reduces the nanofluid flow velocity in the channel and also when the value of Hartmann, Prandtl and Eckert number is low, increasing the Reynolds number increases the maximum value of $\theta$ but when the value of Hartmann, Prandtl and Eckert is high, increasing the Reynolds number reduces the maximum value of $\theta$.
- In general, increasing of Prandtl and Eckert number increases the maximum value of $\theta$ when the Reynolds and Hartmann have a high quantity.

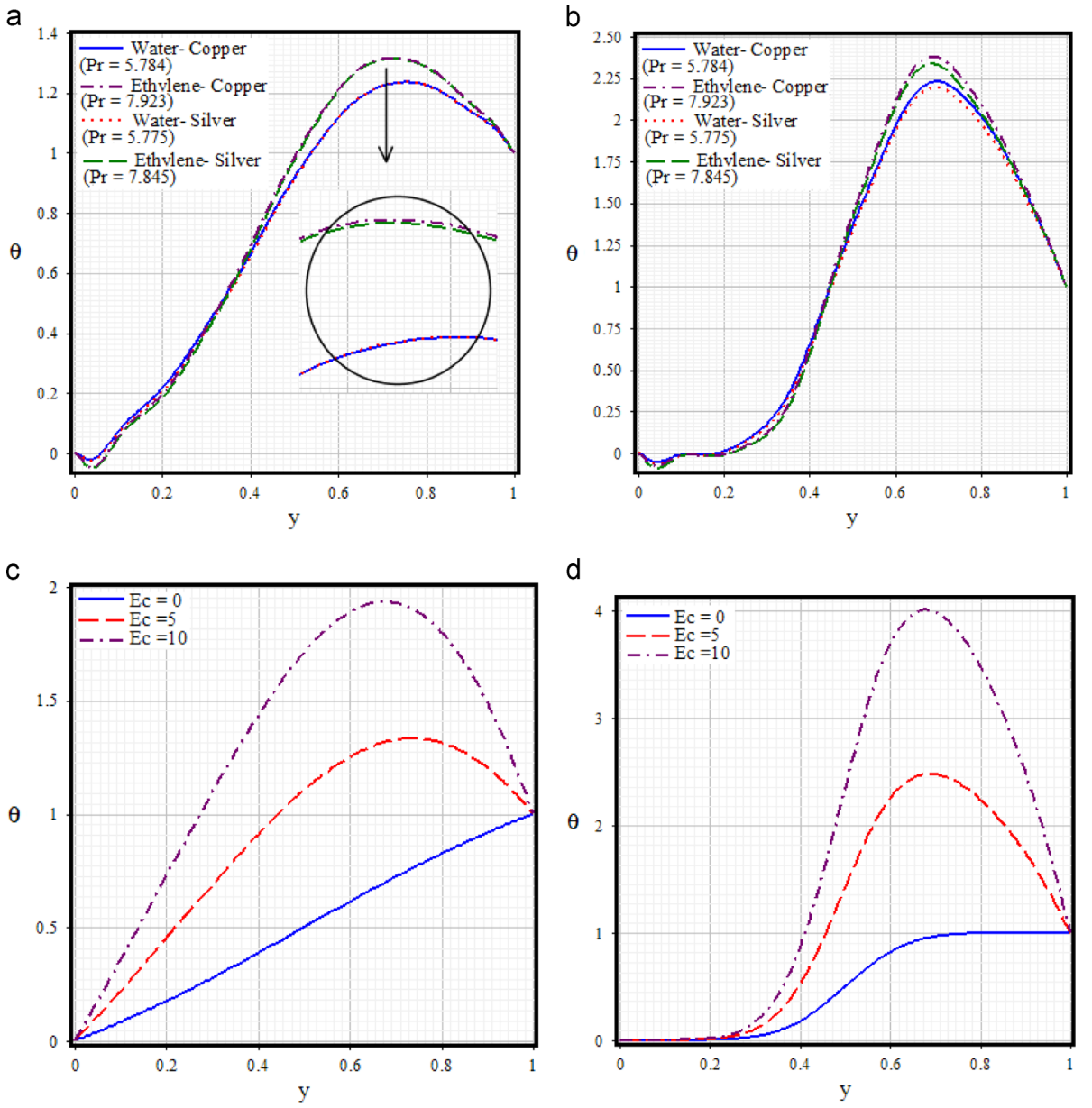


**Fig. 6.** Effect of Prandtl and Eckert numbers on dimensionless temperature for water with copper nanoparticles, $\varphi=0.04$, (a) $\theta(y)$, $Ha=Re=Ec=1$, (b) $\theta(y)$, $Ha=Re=Ec=10$, (c) $\theta(y)$, $Ha=Re=1$, $Pr=5.784$, (d) $\theta(y)$, $Ha=Re=10$, $Pr=5.784$.

## References


[1] Wernert V, Schäf O, Ghobarkar H, Denoyel R. Adsorption properties of zeolites for artificial kidney applications,. Microporous Mesoporous Mater 2005;83:101–13.
[2] Jafari A, Zamankhan P, Mousavi SM, Kolari P. Numerical investigation of blood flow. Part II: In capillaries. Commun Nonlinear Sci Numer Simul 2009;14(4):1396–402.
[3] Goerke AR, Leung J, Wickramasinghe SR. Mass and momentum transfer in blood oxygenators. Chem Eng Sci 2002;57(11):2035–46.
[4] Mneina SS, Martens GO. Linear phase matched filter design with causal real symmetric impulse response. AEU—Int J Electron Commun 2009;63(2):83–91.
[5] Andoh YH, Lips B. Prediction of porous walls thermal protection by effusion or transpiration cooling. An analytical approach. Appl Therm Eng 2003;23(15):1947–58.
[6] Runstedtler A. On themodified Stefan–Maxwell equation for isothermal multi component gaseous diffusion. Chem Eng Sci 2006;61:5021–9.
[7] Berman AS. Laminar flow in channels with porous walls. J Appl Phys 1953;24(9):1232.
[8] Rashidi MM, Freidoonimehr N, Hosseini A, Anwar Bég O, Hung TK. Homotopy simulation of nanofluid dynamics from a non-linearly stretching isothermal permeable sheet with transpiration. Meccanica 2014;49:469–82.

[9] Sheikholeslami M, Domairry D, Ashorynejad HR, Hashim I. Investigation of the laminar viscous flow in a semi-porous channel in the presence of uniform magnetic field using optimal homotopy asymptotic method. Sains Malaysiana 2012;41(10):1177–229.
[10] Soleimani Soheil, Sheikholeslami M, Ganji DD, Gorji-Bandpay M. Natural convection heat transfer in a nanofluid filled semi-annulus enclosure. Int Commun Heat Mass Transf 2012;39:565–74.
[11] Sheikholeslami M, Ashorynejad HR, Domairry G, Hashim I. Flow and heat transfer of Cu–water nanofluid between a stretching sheet and a porous surface in a rotating system. Hindawi Publ Corp J Appl Math 2012;2012:19.
[12] Rashidi MM, Hayatb T, Erfania E, Poura SAMohimanian, Hendi Awatif A. Simultaneous effects of partial slip and thermal-diffusion and diffusion-thermo on steady MHD convective flow due to a rotating disk. Commun Nonlinear Sci Numer Simul 2011;16(11):4303–17.
[13] Domairry D, Sheikholeslami HR, Mohsen Ashorynejad R, Subba R, Gorla, Khani M. Natural convection flow of a non-Newtonian nanofluid between two vertical flat plates. Nanoeng Nanosyst 2012;225:115–22.
[14] Sheikholeslami M, Gorji-Bandpay M, Ganji DD. Magnetic field effects on natural convection around a horizontal circular cylinder inside a square enclosure filled with nanofluid. Int Commun Heat Mass Transf 2012;39(7):978–86.
[15] Sheikholeslami M, Gorji-Bandpy M, Ganji DD, Soleimani S, Seyyedi SM. Natural convection of nanofluids in an enclosure between a circular and a sinusoidal cylinder in the presence of magnetic field. Int Commun Heat Mass Transf 2012;39(9):1435–43.
[16] Sheikholeslami M, Ganji DD, Ashorynejad HR, Rokni HB. Analytical investigation of Jeffery–Hamel flow with high magnetic field and nanoparticle by Adomian decomposition method. Appl Math Mech English Ed 2012;1:25–36 (33).
[17] Rashidi MM, Momoniat E, Ferdows M, Basiriparsa A. Lie group solution for free convective flow of a nanofluid past a chemically reacting horizontal plate in porous media. Math Prob Eng 2014;. http://dx.doi.org/10.1155/2014/239082.
[18] Maxwell JC. A treatise on electricity and magnetism. 2nd ed.Cambridge: Oxford Univ. Press; 435–41.
[19] Sheikholeslami M, Hatami M, Ganji DD. Analytical investigation of MHD nanofluid flow in a semi-porous channel. Powder Technol 2013;246:327–36.
[20] David W Hahn, M. Necati Ozisik, “Heat Conduction,” 2012.